Research Article

Stimulatory Effects of Soluplus® on Flufenamic Acid β-Cyclodextrin Supramolecular Complex: Physicochemical Characterization and Pre-clinical Anti-inflammatory Assessment

Sultan Alshehri,[1,2,4] **Syed Sarim Imam,**[1] **Mohammad A. Altamimi,**[1] **Afzal Hussain,**[1] **Faiyaz Shakeel,**[1] **and Abdulhakeem Alshehri**[3]

Abstract.   The present study demonstrates the solubility and dissolution of flufenamic acid (FLF)/β-cyclodextrin (β-CD)/Soluplus® supramolecular ternary inclusion complex. The binary and ternary inclusion complexes were prepared using solvent evaporation and the microwave irradiation method. The prepared inclusion complexes were evaluated for physicochemical characterization and anti-inflammatory activity using a murine paw edema mol. The phase solubility studies demonstrated 4.59-fold and 17.54-fold enhancements in FLF solubility with β-CD alone and β-CD:Soluplus® combination compared with pure FLF, respectively. The *in vitro* drug release results revealed a significant improvement ($P < 0.05$) in the release pattern compared with pure FLF. Maximum release was found with flufenamic acid binary and ternary complexes prepared using the microwave irradiation method, *i.e.*, $75.23 \pm 3.12\%$ and $95.36 \pm 3.23\%$ in 60 min, respectively. The physicochemical characterization results showed complex formation and conversion of the crystalline form of FLF to an amorphous form. The SEM study revealed the presence of a more agglomerated and amorphous structure of the solid particles, which confirmed the formation of complexes. The anti-inflammatory effect of the complex was higher than pure FLF. Therefore, the FLF:β-CD:Soluplus® inclusion complex may be a very valuable formulation with improved solubility, dissolution, and anti-inflammatory effect.

KEY WORDS: flufenamic acid; inclusion complex; anti-inflammatory activity; solubility enhancement; Soluplus®.

INTRODUCTION

Flufenamic acid (FLF; Fig. 1a) is an anthranilic acid derivative that is used as a nonsteroidal anti-inflammatory drug (1). The chemical formula and molecular weight of FLF are $C_{14}H_{10}F_3NO_2$, and 281.22 g/Mole, respectively. It has potent analgesic, antipyretic, anti-inflammatory activities, and it is used in the treatment of rheumatoid arthritis, osteoarthritis, and other painful musculoskeletal conditions (2). FLF acts *via* the inhibition of cyclooxygenase to prevent the formation of prostaglandins, and it activates transient receptor potential cation channel C6 (3,4). The biopharmaceutical classification system categorized FLF as a class II drug with poor solubility and high permeability (2). It is readily soluble in organic solvents, but it has poor water solubility of 0.0067 mg/mL at 22°C (5,6,7). FLF has the slightly bitter taste and also high rate (30–60%) of gastrointestinal side effects (8,9). There are numerous formulation approaches, such as solid dispersion (10), polyvinyl pyrrolidone dispersion (11), co-crystal (12), and inclusion complex (13), reported to enhance its solubility.

Numerous studies reported the use of a cyclodextrin complex to enhance the solubility of poorly water-soluble drugs (14). Cyclodextrins (CDs) have two different surfaces, *i.e.*, a hydrophilic external surface and a hydrophobic internal cavity. CD molecules have secondary hydroxyl groups on the wider rim and primary hydroxyl groups on the narrow rim, which create the hydrophilicity (15). Among the different CDs, β-CD (Fig. 1b) is the most commonly used parent cyclodextrin due to its large cavity size. It is most suitable for complexing a drug with aromatic rings (16). The formation of
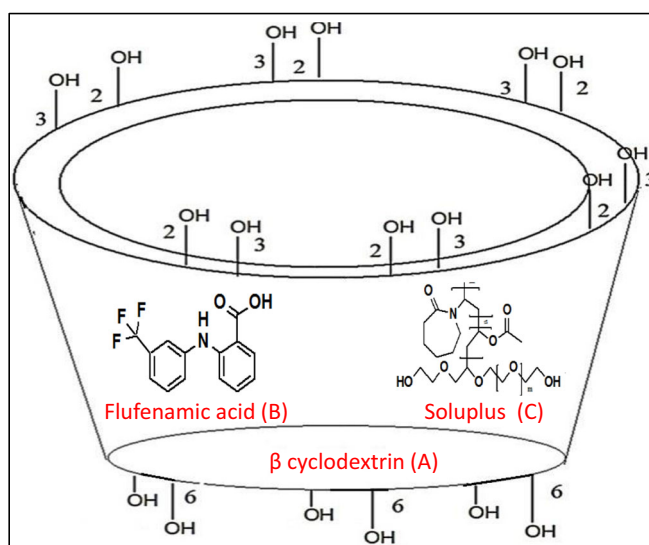
[1] Department of Pharmaceutics, College of Pharmacy, King Saud University, P.O. Box 2457, Riyadh, Saudi Arabia.
[2] College of Pharmacy, Al Marefa University, Riyadh, Saudi Arabia.
[3] Pharmacy, Ministry of Defense, King Abdulaziz Air Base Hospital, Dhahran, Saudi Arabia.
[4] To whom correspondence should be addressed. (e–mail: salshehri1@ksu.edu.sa)

Fig. 1. Chemical structure of **a** flufenamic acid, **b** β-cyclodextrin, and **c** Soluplus®

an inclusion complex with poorly soluble drugs increases drug solubility, dissolution, and bioavailability. It also reduces the gastrointestinal irritancy and masks the bitter taste (15,17).

The addition of auxiliary/ternary substances into the inclusion complex that interact with the CD outer surface ensures the formation of co-complexes, which may provide greater stability constant, complexation efficiency, physicochemical properties, and drug transport compared with binary complexes (18). Soluplus® (Fig. 1c) is a polymeric solubilizer with an amphiphilic nature (19). It has a low critical micellar concentration of $0.76 \times 10^{-3\%}$ *w/v* and 0.8 mg/mL in water (20,21). Soluplus® is soluble in water and exhibits a greater solubility in many organic solvents (22). It helps in maintaining stability by reducing crystal nucleation and growth (23,24). Soluplus® may be used in the formulation of inclusion complexes to achieve higher solubility, dissolution, and bioavailability (25). It also helps in the formation of poly(pseudo) rotaxane with CDs and their derivatives (21). The literature reports prolonged drug permeation at the application site with the use of the combination of amphiphilic copolymers and CDs (26,27). Over the years, researchers demonstrated that the use of Soluplus® (as ternary substance) with CDs enhanced the solubility and *in vivo* drug absorption of insoluble drugs. A flurry of research studies were published on the improvements in solubility and dissolution with the combination of Soluplus® and CDs for drugs, such as Carvedilol (21), itraconazole (22,25), tacrolimus (24), Natamycin (26), carbamazepine (28), and docetaxel (29). These studies reported that the addition of Soluplus® in the inclusion complex as a ternary substance significantly enhanced drug solubility, dissolution, and bioavailability.

The hypothesis of the present work was designed to enhance the solubility of FLF with the addition of β-CD and Soluplus®. FLF is a BCS class II category drug and shows poor water solubility, dissolution, and bioavailability. It may also undergo precipitation due to first-pass metabolism. Improvements in the solubility, dissolution, and inhibition of drug precipitation may enhance the bioavailability. The current study prepared FLF

binary and ternary inclusion complexes. The prepared complexes were characterized in a solubility study, dissolution study, solid-state characterization, NMR spectroscopy study, and an *in vivo* paw edema anti-inflammatory activity in a murine model. To the best of our knowledge, the effects of Soluplus® on the FLF:β-CD complex were not examined. Therefore, the present study may have greater significance in the future for the formulation of ternary FLF complexes using β-CD and the Soluplus® blend.

MATERIAL AND METHODS

Materials

Flufenamic acid (FLF; purity 99.5%) was purchased from Sigma Aldrich (St. Louis, MO, USA), and Soluplus® (118,000 g/mol) was received as a gift sample (BASF SE, Germany). Beta-cyclodextrin (β-CD) was obtained from Sigma, Germany. Sodium CMC was obtained from BDH Chemicals Ltd., England. All other chemicals used were of analytical grade.

Methods

Phase Solubility Studies

These studies were performed to select the stoichiometry of FLF - β-CD and FLF - β-CD - Soluplus® using the described method by Higuchi-Connors (30). Briefly, different concentrations of β-CD solutions (2–12 mM) were prepared, and an excess quantity of FLF was added to the solution. Similarly, β-CD solutions (2–12 mM) with the addition of Soluplus® (0.006 mM) concentration were prepared, and excess of FLF was added the solution. The flasks were kept on a mechanical shaker for 72 h, and the temperature of the study was maintained at 25°C. The supernatant was collected from the flasks and filtered using a membrane filter (0.22 μm). FLF content ($n = 3$) was analyzed using a UV spectrophotometer at 286 nm.

Table I. Formulation Design of Flufenamic Acid Inclusion Complex Using Different Methods

Flufenamic binary complex (mM ratio)			Flufenamic ternary complex (mM ratio)		
Physical mixture	Solvent evaporation	Microwave irradiation	Physical mixture	Solvent evaporation	Microwave irradiation
FLF:β-CD 1:1	FLF:β-CD 1:1	FLF:β-CD 1:1	FLF:β-CD:Soluplus® 1:1:0.006	FLF:β-CD:Soluplus® 1:1:0.006	FLF:β-CD:Soluplus® 1:1:0.006

The stability constants (Kc) were also calculated from the phase solubility graph using the following formula:

$$Kc_0slope/So\ (1-slope) \tag{1}$$

where Kc = stability constant; So = solubility of FLF in water.

Complexation efficiency (CE) was also calculated to determine the capacity of CDs to form an inclusion complex with hydrophobic drugs. It was calculated using the formula:

$$CE_0slope/(1-slope) \tag{2}$$

Binary and Ternary Complex Formulation

The complexes between FLF - β-CD and FLF - β-CD - Soluplus® were prepared using two different methods (solvent evaporation (SE), microwave irradiation (MI)). The previously sieved (#80 mesh) powder samples were weighed for the binary complex (FLF - β-CD) and the ternary complex (FLF - β-CD - Soluplus®) were used to prepare the supramolecular complex (Table I).

Physical Mixture

The binary physical mixture (FLF - β-CD) and ternary physical mixture (FLF - β-CD - Soluplus®) were prepared *via* a thorough mixing of each component. Accurately weighed quantities of samples were triturated and mixed thoroughly in a mortar and pestle (Table I). The prepared physical mixtures (760 mg) were again sieved through #80 mesh and kept in a desiccator for further use.

Solvent Evaporation Method

The FLF-BCSE and FLF-TCSE were prepared using the SE method using FLF and carriers as shown in Table I. The calculated and weighed amount of FLF was dissolved in ethanol, and β-CD was dissolved in water (ethanol:water, 1:1 *v/v*, 4 mL). The β-CD solution was added slowly to the FLF-ethanol phase with continuous stirring. The solvent was evaporated until a dried mass was formed and further kept in a vacuum oven at a temperature of 50°C for 48 h for the complete removal of solvents (31). Similarly, FLF-TCSE was prepared with the addition of Soluplus® to the FLF β-CD complex. The prepared powder samples were dried, milled, and passed through a sieve (#80 mesh) to get a uniform, fine particle, which was stored in desiccator for further use.

Microwave Irradiation Method

Accurately weighed samples of FLF:β-CD (FLF-BCMI) and FLF:β-CD:Soluplus® (FLF-TCMI) were taken in a beaker (Table I). The weighed quantity of drug and carrier for the binary complex were added to ethanol:water (1:1 *v/v*, 4 mL) to make a homogenous paste. The prepared sample was kept in a microwave oven (Samsung ME0113M1; Malaysia) for microwave irradiation at 700 W and 50°C for 4 min (32). Similarly, FLF-TCMI was prepared with the addition of Soluplus® to the FLF β-CD complex. The samples were collected and allowed to cool at room temperature. The dried sample was milled and sieved through a #80 mesh to get a uniform and fine-sized sample, which was stored in a desiccator for further use (33).

Solubility Studies

The solubilities of FLF, FLF-BPM, FLF-TPM, FLF-BCSE, FLF-BCMI, FLF-TCSE, and FLF-TCMI were performed in 0.1N HCl and water. Briefly, weighed samples were added to the measured volume of 0.1N HCl and water in a conical flask. FLF suspensions were mechanically shaken for 72 h at 25°C and filtered through the membrane filter. The samples were diluted, and the absorbance was measured at 286 nm using a spectrophotometer in triplicate ($n = 3$).

In Vitro Drug Release Studies

These studies were performed for pure FLF, FLF-BPM, FLF-TPM, FLF-BCSE, FLF-BCMI, FLF-TCSE, and FLF-TCMI to evaluate FLF release. The study was performed using dissolution media 0.1N HCl (pH 1.2; 900 mL) at a temperature of 37 ± 0.5°C with 100 rpm (34). The samples containing FLF (equivalent to 10 mg) and pure FLF (10 mg) were placed into the release medium. The released samples (5 mL) were removed from the flask at fixed time intervals and replenished with the same volume. The samples were filtered, diluted, and quantified for FLF content at 286 nm using a spectrophotometer. The release profile was further used to check the release mechanism *via* plotting of the data into different release kinetic models using PCP Disso V3 software (Bharati Vidyapeeth Deemed University, Pune, Maharashtra, India). The data showed the best linear fit, and the highest R^2 value was selected as the kinetic model (35,36). The similarity factor (f_2) calculated from Eq. (3) was used to compare the resulting release profiles (37).

$$\text{Similarity factor} = 50 \times \text{Log} \left[1 + \left(\frac{1}{n} \right) \sum_{k=1}^{n} n(Rt-Tt)^2 \right]^{-0.5} \times 100 \quad (3)$$

where Rt and Tt were defined as API % dissolved at time t, the reference (R) and test samples (T). The release profiles were considered equal when f_2 was higher than 50. The average difference between the two profiles at all-time points was > 10%.

Differential Scanning Calorimetry

The transformations of drugs that changed during the formulation were evaluated using DSC (Perkin Elmer 8000; Shelton, CT, USA). The drug (pure FLF), carriers (β-CD, Soluplus®), and prepared formulations (FLF-TPM, FLF-TCMI, and FLF-TCSE) were examined for transformations in state. The samples (~ 2.0 mg) were taken in an aluminum pan and scanned at a heating rate of 10°C/min in the temperature range of 55–310°C.

X-ray Diffraction

The drug (pure FLF), carriers (β-CD, Soluplus®), and prepared formulations (FLF-TPM, FLF-TCMI, and FLF-TCSE) were performed to assess the drug transformation. The changes in the peak intensity and the representative diffraction peaks were evaluated using X-ray diffractometer (Ultima IV diffractometer, Rigaku, Japan).

Fourier Transformed Infrared Spectroscopy

This study was performed to check the formation of complex by evaluating deviations in peak shape, position, and intensity. The spectra of the drug (pure FLF), carriers (β-CD, Soluplus®), and prepared formulations (FLF-TPM, FLF-TCMI, and FLF-TCSE) were evaluated using an IR spectrophotometer (ATR-FTIR, Bruker Alpha, Germany). The samples were scanned in the range of 450–4000 cm^{-1}, and an interpretation of spectra was performed to check any conformational changes.

Nuclear Magnetic Resonance

Quantitative analysis was used to determine the molecular conformation and physical properties of the pure compounds and their formulations. The purity and interactions between drug (pure FLF), carriers (β-CD, Soluplus®), and prepared formulations (FLF-TPM, FLF-TCMI, and FLF-TCSE) were assessed using ^{1}H NMR (700 MHz) and ^{13}C NMR (125.6 MHz; Bruker NMR; software topspin 3.2) studies. The study was performed using deuterated dimethyl sulfoxide using tetramethyl silane as an internal standard.

Scanning Electron Microscope

The surface morphologies of drug (pure FLF), carriers (β-CD, Soluplus®), and prepared formulations (FLF-TPM, FLF-TCMI, and FLF-TCSE) were evaluated using a JSM 6360A microscope (JOEL, Tokyo, Japan). A thin layer of gold was used to coat the samples, which were visualized under an electron microscope to check morphology.

Anti-inflammatory Activity

The activity of pure FLF and FLF-TCMI was examined using a carrageenan-induced rat paw edema method (38,39). The protocol for these studies was reviewed and approved by the "Animal Ethics Committee of King Saud University, Riyadh, Saudi Arabia (approval number KSU-SE-19-19)." Eighteen male Wistar rats (weight 220–250 g) were procured from the "Pharmacy Experimental Animal Care Center (King Saud University, Riyadh, Saudi Arabia)." The animals were divided into three different groups: group I (control), group II (FLF-TCMI), and group III (pure FLF). Each group contained six rats ($n = 6$). All of the rats were housed together in a standard animal room with free access to "Lipton feed and water *ad libitum*." Paw edema was induced using (0.1 mL) a carrageenan injection (1.0% *w/v*), which was injected subcutaneously into the left hind paw (2). The animals were fasted overnight before receiving any treatment. The samples were prepared in a sodium carboxy methyl cellulose (Na-CMC) suspension (0.1% *w/v*), which was administered orally *via* gavage. Paw edema was evaluated at different time intervals to investigate the anti-inflammatory efficacy. Thirty minutes after carrageenan injection, pure FLF and FLF-TCMI (10 mg/kg) were administered orally (2). The paw volumes before (0 h) and after carrageenan injection (1, 2, 4, and 6 h) were measured using a "Digital Plethysmometer (Ugo, Italy)." The anti-inflammatory activity of pure FLF and FLF-TCMI was determined as per reported in the literature (39).

Statistical Analysis

The values for the anti-inflammatory studies are expressed as the means ± SD of six independent experiments. Comparisons were performed using Student's t test in MS Excel 2016, and the value of P 0.05 was taken as the significance value.

RESULTS AND DISCUSSION

Phase Solubility Studies

The phase solubility diagrams of the binary and ternary system were evaluated, and the results showed an A_L-type graph (Fig. 2). The best stoichiometric ratios were found between FLF:β-CD (1:1) and FLF:β-CD:Soluplus® (1:1:0.006). The binary complex showed a Kc value of 255.47 M^{-1} and CE of 4.59, and the ternary complex depicted a Kc value of 975.49 M^{-1} with CE of 17.54. These values confirm the formation of a stable complex and improved the complexation efficiency of β-CD. Complexes with Kc values between 100 M^{-1} and 1000 M^{-1} represent ideal complex formation. Less than 100 M^{-1} represents unstable drug/CD complexes, and greater than 1000 M^{-1} may deleteriously affect the absorption of the drug (40). The presence of Soluplus® in the complex enhances the effect *via* externally adhering to the CD surface, which helps in the formation of a co-complex that could lead to higher Kc values (41).

Solubility Studies

The reported solubilities of pure FLF were 9.09 μg/mL and 48.6 μg/mL in water and 0.1N HCl, respectively (12,42). Alshehri et al. also reported a solubility ~ 9.1 μg/
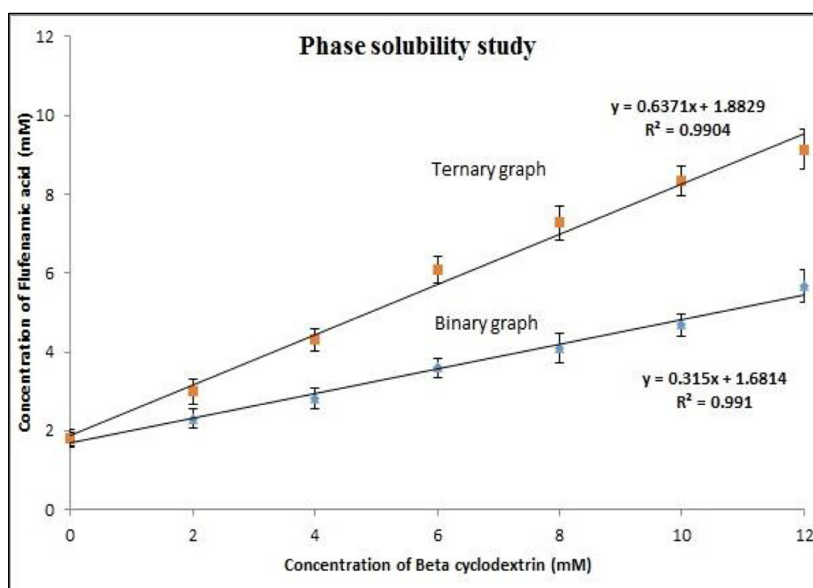
Fig. 2. Phase solubility of binary complex (FLF with β-CD) and ternary complex (FLF with β-CD and Soluplus®)

mL in water at room temperature (7). The solubility of pure FLF was 7.8 ± 0.0011 μg/mL in water and 45.1 ± 0.0047 μg/mL in 0.1N HCl (pH 1.2) in our study. The findings of the present study are closer to the reported values in the literature. The solubility of FLF in binary and ternary complexes increased significantly compared with pure FLF. The binary complexes prepared using the SE and MI methods showed 9.23- to 14.42-fold enhancement in aqueous solubility and 8.11- to 15.73-fold enhancement in 0.1N HCl (pH 1.2). The ternary complex showed 23.12- to 31.65-fold solubility enhancement in water and 20.11- to 35.34-fold enhancement in 0.1N HCl

(pH 1.2). The addition of Soluplus® with β-CD in the ternary inclusion complex produced a noticeable synergistic effect in increasing the solubility compared with the binary complex. Among the different FLF complexes, the FLF complex prepared using the MI method showed the highest solubility for binary and ternary systems. The addition of a ternary substance in the drug CD complex induces an interaction with the hydrophobic portion of β-CD. The direction of the hydrophilic part of Soluplus® towards the drug and CD decreases the surface tension and leads to enhanced aqueous solubility (43).
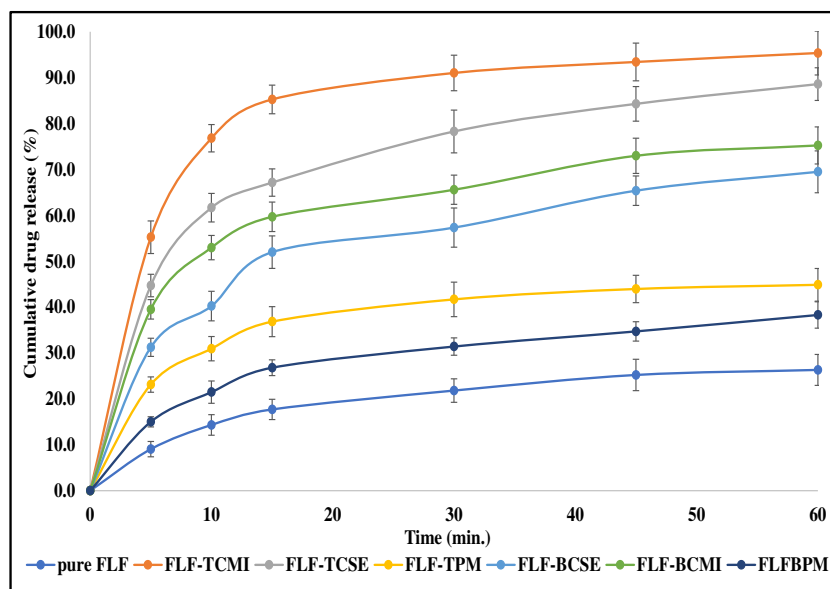
Fig. 3. *In vitro* drug release profile of pure FLF, physical mixture (binary and ternary), binary inclusion complex (SE and MI), and ternary inclusion complex (SE and MI). Values are presented as means ± SD with triplicates

In Vitro Drug Release

A sink condition is the ability of the release media to dissolve a drug at least three to four times the total sample (44). The release study was performed in 0.1N HCl, and the practical solubility of FLF was 45.1 mg/L. Improvements in release were found in the following order: FLF-TCMI > FLF-TCSE > FLF-BCMI > FLF-BCSE > FLF-TPM > FLF-BPM > pure FLF (Fig. 3). Pure FLF showed a poor drug release profile of $26.12 \pm 1.12\%$ in 60 min. FLF-BPM showed $38.11 \pm 3.12\%$ release in 60 min, and FLF-TPM showed $44.86 \pm 2.34\%$ release in 60 min. The enhancement in release may be due to the improvement in the solubility of FLF in the presence of Soluplus® as a ternary substance in the physical mixture (45). FLF-BCSE and FLF-BCMI showed $69.48 \pm 3.23\%$ and $75.18 \pm 3.11\%$ FLF release, respectively, which are significantly higher than pure FLF, and binary and ternary physical mixtures. The higher FLF release may be due to the partial entrapment of drug molecules inside the β-CD torus and hydrophilic nature (46). FLF-TCSE and FLF-TCMI showed $88.95 \pm 2.89\%$ and $95.12 \pm 4.21\%$ release in 60 min, respectively.

This finding may be due to the addition of Soluplus® as a ternary substance. The presence may help achieve better inclusion, complexation efficiency, and amorphization by microwave rays, which led to enhanced drug release ($95.12 \pm 4.21\%$) within the examined period of time. Notably, there was a slight difference in drug release (6.17%) between the TCSE and TCMI methods. The inclusion complex prepared using the MI method showed greater release than the SE method. The microwave penetration allows the production of heat throughout the sample at the same rate, which results in uniform volumetric heating. This methodology provides better intimate contact of FLF with Soluplus® and β-CD (36,46).

The formulation was also evaluated for $T_{50\%}$ and $T_{90\%}$, and the results are depicted in Table II. FLF-TCSE and FLF-TCMI showed $T_{50\%}$ in less than 6 min., and FLF-BCSE and FLF-BCMI showed $T_{50\%}$ values 14.2 and 8.8 min, respectively. The $T_{90\%}$ value of FLF-TCMI occurred at 28.22 min only. The release data were fitted to different release kinetics model, and the correlation coefficient (R^2) values were maximum for first-order kinetics (Table II). The similarity factors f_2 were calculated and compared with each other to identify significant differences. The release curves for the binary complex showed f_2 values less than 50. The addition of Soluplus® in the ternary complex showed f_2 values greater than 50, which confirms that all of the curves were different from pure FLF.

Differential Scanning Calorimetry

Differential scanning calorimetry was used to confirm complex formation of FLF with β-CD and Soluplus®, as depicted in Fig. 4. The thermal curve of pure FLF and β-CD showed sharp endothermic peaks at 134.66°C (area = 481.497 mJ) and 298.34°C (area = 495.652 mJ), respectively, which are analogous to their melting points. The endothermic peak of FLF retained the same temperature of 134.46°C in TPM, but the peak area was significantly reduced (area = 105.603 mJ). The change in the endothermic peak was due to a weak or no interaction between FLF, β-CD, and Soluplus® in FLF-TPM (47). FLF-TCSE and FLF-TCMI also showed very short and broad endotherm peaks at 133.37°C (area = 18.213 mJ) and 133.69°C (area 34.177 mJ), respectively. The area and delta H was significantly reduced in both samples compared with FLF-TPM. This result may be due to the higher solubility of FLF and conversion to an amorphous form in the presence of β-CD and Soluplus®. The FLF-TCSE and FLF-TCMI ternary complexes also showed a decrease in the dehydration enthalpy. Substitution of the water molecules in the β-CD cavity from FLF-TCSE and FLF-TCMI altered the energy states of these preparations. The presence of Soluplus® in the formulation facilitated the exchange of water molecules due to its hydrophilic nature.

X-ray Diffraction

The crystallinity of FLF in the inclusion complex was determined *via* comparisons of the characteristic peaks and peak intensities of pure FLF and the FLF inclusion complexes. The diffractograms of the drug (pure FLF), carriers (β-CD, Soluplus®), and prepared formulations (FLF-TPM, FLF-TCMI, and FLF-TCSE) are shown in Fig. 5. The FLF diffractogram showed characteristic peaks at diffraction angles of 17.9°, 19.0°, 24.6°, 27.5°, and 30.8°, which indicates its crystalline property (10). FLF-TPM showed a partial loss of the crystalline nature of FLF with low peak intensities. However, the ternary complexes FLF-TCMI and FLF-TCSE showed marked changes in peak intensities and patterns. The sharp peaks transformed into small and broad peaks. Changes in the peaks were due to the conversion of crystalline FLF into an amorphous state with the SE and MI methods.

Table II. Release Kinetics Model of Flufenamic Acid Physical Mixture and Inclusion Complex

Release model	FLF-BPM	FLF-BCMI	FLF-BCSE	FLF-TPM	FLF-TCMI	FLF-TCSE
Zero order model	0.8712	0.8910	0.8692	0.8344	0.9265	0.8932
1st order model	0.9167	0.9817	0.9782	0.9332	0.9478	0.9797
Matrix model	0.7607	0.8445	0.8322	0.8143	0.6715	0.9029
Peppas model	0.8847	0. 8688	0.9126	0.8870	0.8987	0.9883
Hix.Crow. model	0.8427	0.7677	0.8604	0.9237	0.9012	0.7376
$T_{50\%}$ (min)	-	8.8 min	14.2 min	-	4.1 min	5.8 min
$T_{90\%}$ (min)	-	-	-	-	29.2 min	-

FLF, flufenamic acid; *BPM*, binary physical mixture; *TPM*, ternary physical mixture; *BMI*, binary microwave irradiation; *TMI*, ternary microwave irradiation; *BSE*, binary solvent evaporation; *TSE*, ternary solvent evaporation
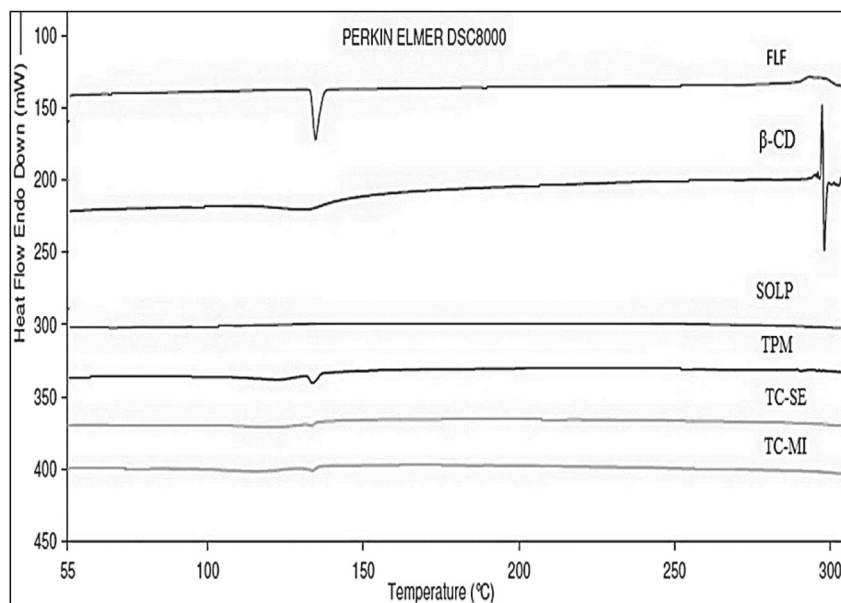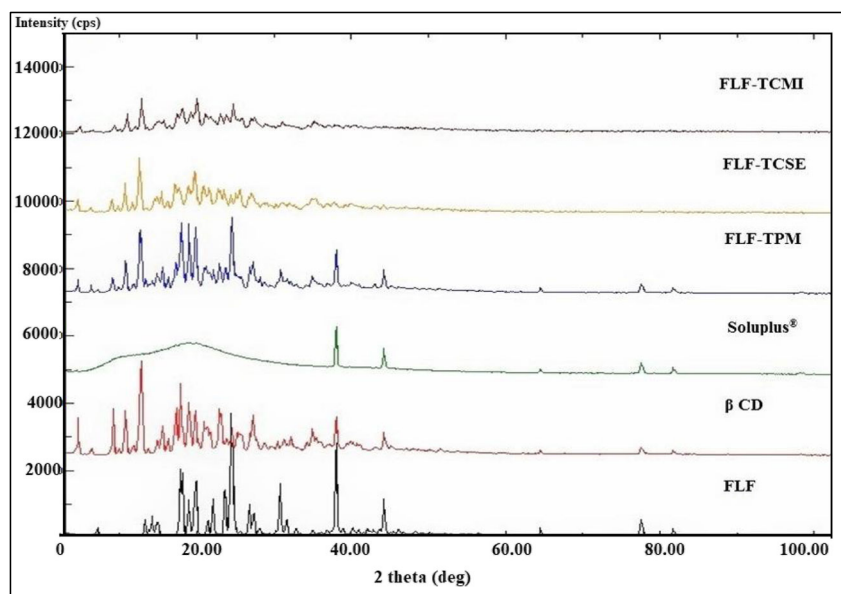
Fig. 4. Differential scanning calorimetry of flufenamic acid, β-CD, Soluplus®, ternary physical mixture, ternary inclusion complex (SE), and ternary inclusion complex (MI)

Fourier Transformed Infrared Spectroscopy

The characteristic IR frequencies of the drug (pure FLF), carriers (β-CD, Soluplus®), and prepared formulations (FLF-TPM, FLF-TCMI, and FLF-TCSE) with the chemical bonds responsible for the corresponding stretching frequencies are depicted in Fig. 6. FLF showed a spectral peak for N–H stretching (3313.59 cm^{-1}) and the characteristic carboxylic

frequencies for β-CD were identified at 3277.42, 1020.04, and 1413.18 cm^{-1}, which reflect the stretching vibration of O–H and C–O–C and the bending vibration for the CH$_2$ moiety. C–O stretching of the secondary alcohol was recorded in the region of 1149.51 cm^{-1}. The most distinct peaks for Soluplus® were the stretching vibration at 2923.10 cm^{-1} for tertiary nitrogen and 1731.97 cm^{-1} for the carbonyl moiety. A cluster of other peaks were observed at 1627.90, 1236.08, and

Fig. 5. X-ray diffraction spectra of flufenamic acid, β-CD, Soluplus®, ternary physical mixture, ternary inclusion complex (SE), and ternary inclusion complex (MI)

acid stretching peak at 2863.87 cm^{-1}. Other peaks were also observed at 1656.00 cm^{-1} for C=C stretching and 1024.80 cm^{-1} for C–F stretching. The characteristic

1025.17 cm^{-1} for ester, alcohol, and the C–O–C moiety, respectively. A bending vibration was also observed at 1431.24 cm^{-1} for the CH$_2$ moiety in the carrier.
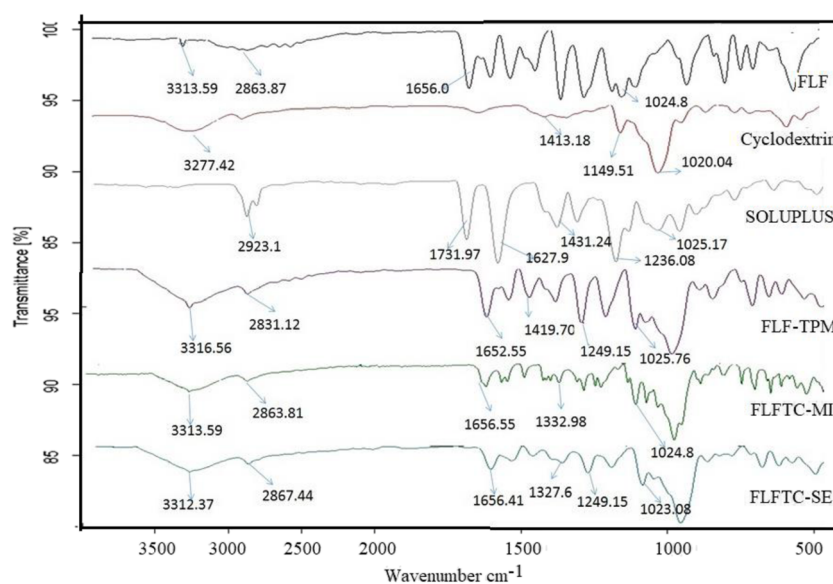
Fig. 6. Infrared spectra of flufenamic acid, β-CD, Soluplus®, ternary physical mixture, and ternary inclusion complex (SE and MI)

The ternary physical mixture (FLF-TPM) and ternary inclusion complexes (FLF-TCSE and FLF-TCMI) showed the presence of a carboxylic acid hydroxyl peak, as observed with pure FLF. There was a slight variation in the peaks for C=C and NH stretching, which corresponded to 1652.55 and 3316.56 cm^{-1}, respectively. The peaks for C–O–C stretching vibrations occurred at 1025.76 cm^{-1} and 1249.15 cm^{-1} from the used carriers. Further CH$_2$ bending vibrations were observed at 1419.70 cm^{-1}. Stretching vibrations at the 1024.80 and 3313.59 cm^{-1} peaks were also observed for C–F and NH in FLF-TCMI. FLF-TCSE also exhibited the presence a C–F peak, but a slight deviation in the stretching of NH peaks at 3312.37 cm^{-1} was observed.

Carrier peaks were also observed at 1327.60 and 1332.98 cm^{-1} for the CH$_2$ bending vibration, and C=C stretching vibrations occurred at 1656.41 and 1656.00 cm^{-1} for FLF-TCSE and FLF-TCMI, respectively. The C–O–C stretching peaks were absent in FLF-TCMI but present in FLF-TCSE at 1023.08 cm^{-1}. These results confirmed that FLF-TCMI showed enhanced solubility compared with FLF-TPM and FLF-TCSE. The above spectral studies also showed no interaction between pure FLF and carriers.
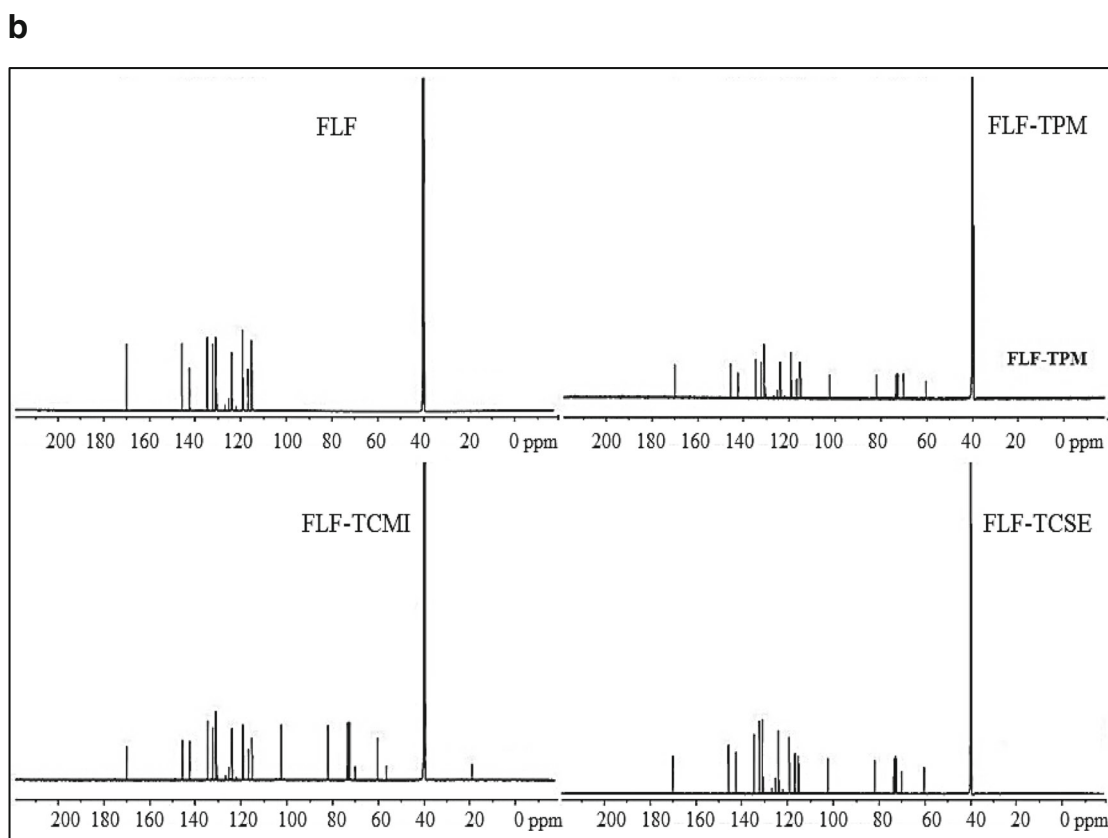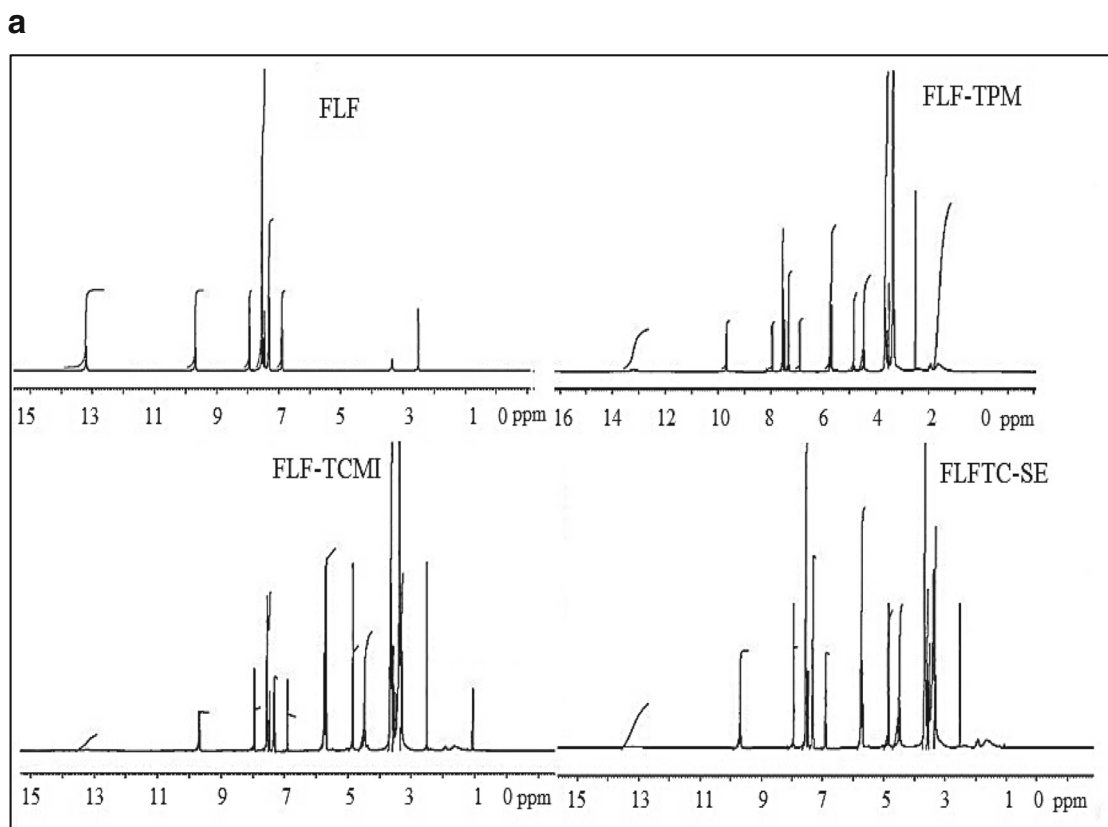
Nuclear Magnetic Resonance

The ^{1}H-NMR and ^{13}C NMR spectra of pure FLF, FLF-TPM, FLF-TCMI, and FLF-TCSE were studied to analyze the interactions between pure FLF and carriers (β-CD and Soluplus®) using the chemical shift (δ), as depicted in Fig. 7a, b. The δ values of ^{1}H NMR spectra of pure FLF (Fig. 7a), β-CD (Figure S1a), and Soluplus® (Figure S1b), were compared with FLF-TPM, FLF-TCMI, and FLF-TCSE.

In ^{1}H NMR spectra (Fig. 7a), the δ values of pure FLF, β-CD, and Soluplus® were compared with prepared samples of FLF-TPM, FLF-TCMI, and FLF-TCSE. The ^{1}H NMR spectrum of FLF in DMSO-$d6$ exhibited a marked deshielded singlet at 13.21 ppm, which was ascribed to the carboxyl proton at the C-6 position. The aromatic 8H carbon at C-2, 3,

4, 5, 9, 11, 12, and 13 exhibited multiplet peaks at 6.89–7.95, and a singlet peak was also observed for the NH at position 1, with a δ value of 9.69 ppm.

In contrast, the complexes FLF-TPM, FLF-TCMI, and FLF-TCSE revealed absolutely unnoticeable changes in the chemical shift values of aromatic rings and nitrogen peak (–NH), with a multiplet δ value of 6.89–7.95 ppm and a singlet peak of δ 9.69 ppm, respectively. A minor change was observed for the carboxylic peak (–COOH) at δ values of 13.20 for FLF-TPM, 13.23 for FLF-TCMI, and 13.22 ppm for FLF-TCSE. The presence of carboxylic peaks in formulations was also confirmed in IR spectral values. The slight variation may be due to the presence of the used carrier in the inclusion complex. The ^{1}H NMR results of FLF-TCMI and FLF-TCSE showed that the β-CD and Soluplus® peaks underwent immense alterations, which indicates its importance in the solubility amplification of FLF. The broad cyclic heptane peak at δ 1.66–1.93 ppm of Soluplus® and singlet peak at δ 2.41 ppm for the hydroxyl group of β-CD were also present in complexes with a slight deviation at δ 2.51 ppm, which is also consistent with the IR spectral values. This result supports the important role of the interaction of cyclic heptanes and hydroxyl groups in the complex formation that leads to enhanced FLF solubility. The presence of the carboxylic group of pure FLF and the hydroxyl group of β-CD in complexes with slight chemical shifts also indicates the formation of complexes. The aromatic protons of FLF showed a significant upfield shift in the presence of β-CD. The presence of a hydroxyl group in complexes indicates that the C-2 protons of FLF are located in close proximity to the oxygen atoms in the β-CD cavity, which is rich in electrons ([47,48]). Furthermore, the presence of β-CD glucose peaks at δ 5.74–3.31 ppm was also observed in complexes with minor changes in chemical shift values, which confirms the formation of complexes.

In ^{13}C NMR (Fig. 7b), extra peaks were observed for FLF-TCSE with δ values of 60.78 and 72.18 ppm and FLF-TCMI with a δ value of 56.50, which may be due to β-CD or

a

b

Fig. 7. **a** Nuclear magnetic resonance spectra (C^{13}) of flufenamic acid, ternary physical mixture, and ternary inclusion complex (SE and MI). **b** Nuclear magnetic resonance spectra (^1H) of flufenamic acid, ternary physical mixture, and ternary inclusion complex (SE and MI)
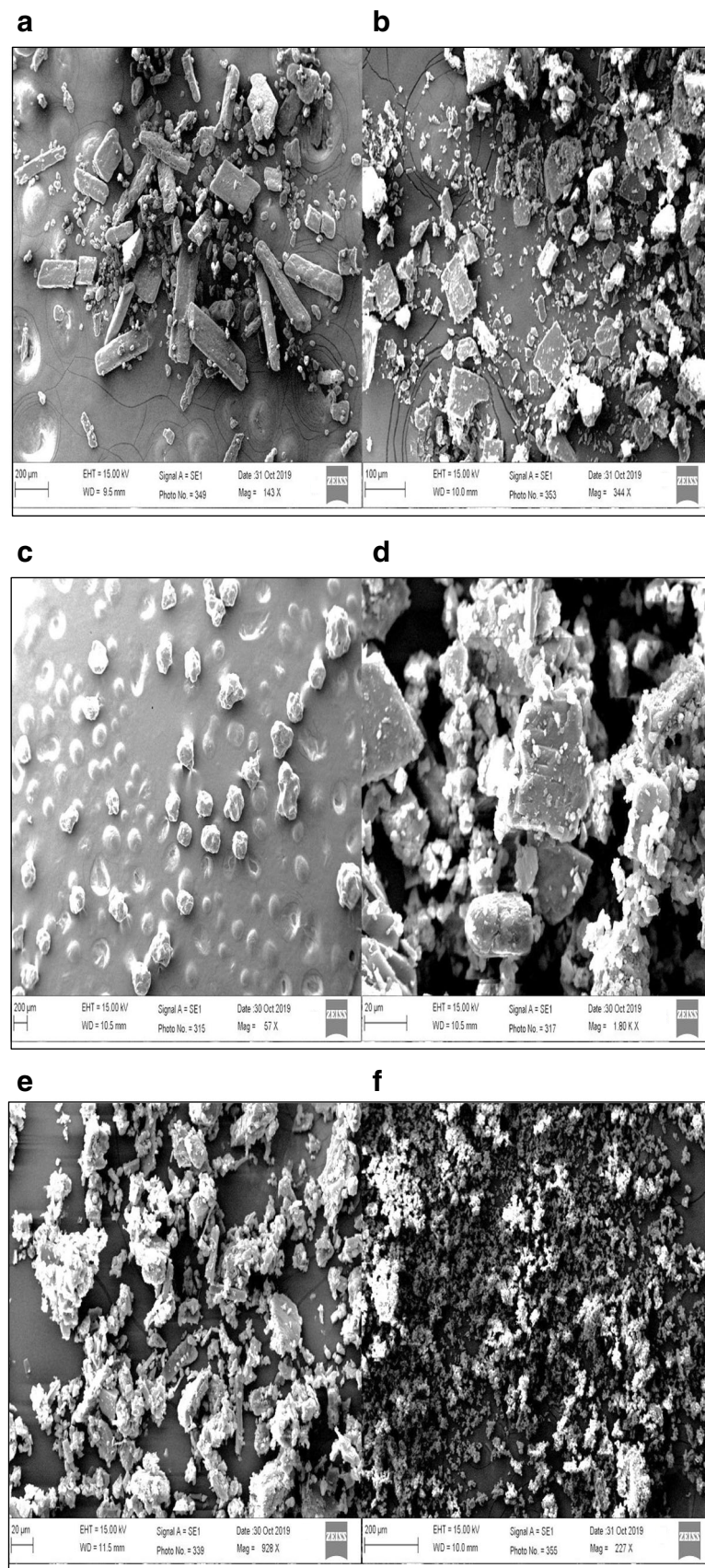
Fig. 8. Scanning electron microscopy of **a** flufenamic acid, **b** β-CD, **c** Soluplus®, **d** ternary physical mixture, **e** ternary inclusion complex (SE), and **f** ternary inclusion complex (MI)
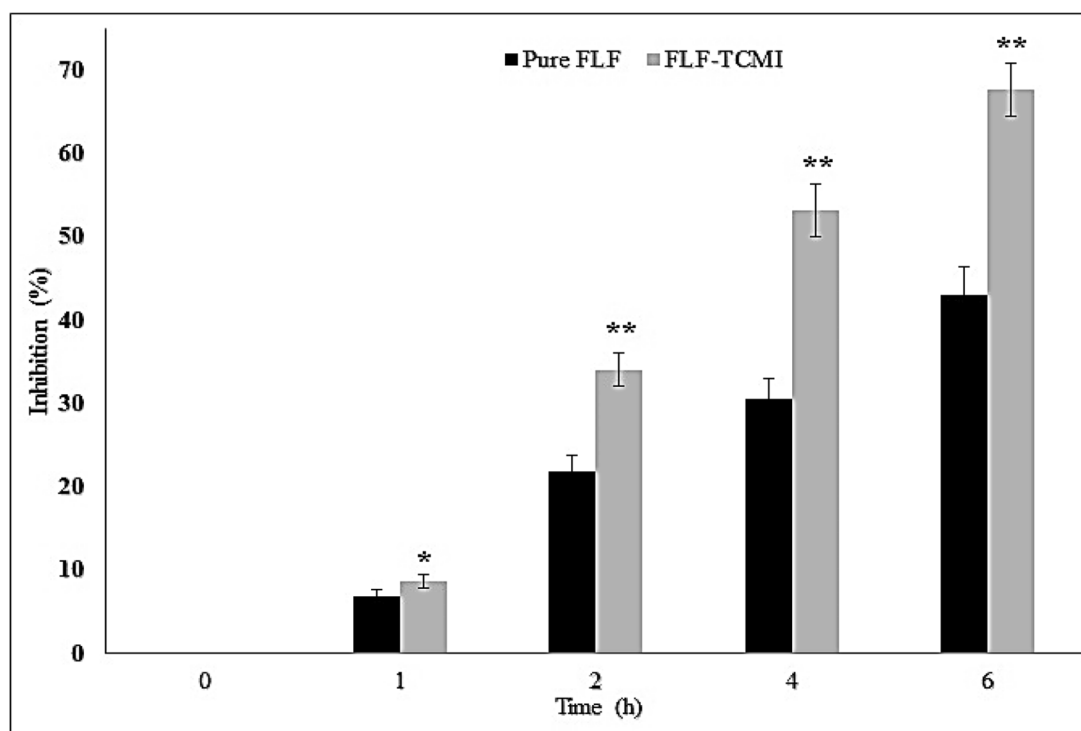
Fig. 9. Comparative *in vivo* anti-inflammatory activity profile of FLF and FLF ternary inclusion complex (MI). Data are means ± SD of six rats in each group, double asterisks indicate significant difference from pure FLF ($P < 0.05$), single asterisk indicates not significant difference to pure FLF (P 0.05)

Soluplus®. A slight variation was observed for FLF-TCMI and FLF-TCMI with δ values of 40.44 and 40.45 ppm, in contrast to β-CD and Soluplus®. The above peaks were missing in FLF-TPM. In conclusion, we propose that the ^{13}C NMR spectra of FLF-TCMI and FLF-TCSE support modification in the arrangement of molecules to intensify the solubility of pure FLF.

The NMR spectra, IR spectra, DSC thermograms, and XRD images confirm the formation of complexation. There was a chemical shift in the NMR study, and IR studies revealed modification in the inclusion complex spectra. DSC and XRD revealed the conversion of FLF from a crystalline state to an amorphous state in the inclusion complex. The stability constant, solubility, and dissolution results also confirmed the formation of complexes. There were significant enhancements in solubility and dissolution from the inclusion complex.

Scanning Electron Microscopy

Figure 8 illustrates the SEM micrographs of FLF, β-CD, Soluplus®, FLF-TPM, FLF-TCMI, and FLF-TCSE. FLF showed an easily identified defined shaped crystal (Fig. 8a). The images of β-CD (Fig. 8b) and Soluplus® (Fig. 8c) showed amorphous particles that resembled a spherical ball (31). FLF-TPM showed the presence of FLF crystals mixed with the particles of β-CD (Fig. 8d). The size of the crystals was reduced due to processing, but some agglomerates were observed with sparse unmodified FLF crystals. The FLF-TCMI and FLF-TCSE prepared using the SE and MI methods showed an absence of FLF crystal structure. The

presence of more agglomerated and amorphous structures confirmed the formation of complexes (Fig. 8e, f).

Anti-inflammatory Activity

FLF is a water-insoluble drug that shows poor dissolution and bioavailability. Due to first-pass metabolism, FLF may undergo precipitation in the small intestine. Therefore, the anti-inflammatory activity was assessed for the selected inclusion complex formulation (FLF-TCMI) on the basis of its maximum solubility and dissolution. The *in vivo* anti-inflammatory efficacies of FLF-TCMI compared with pure FLF are presented in Fig. 9. The anti-inflammatory activity of pure FLF and FLF-TCMI increased over time. The anti-inflammatory activity of FLF-TCMI in terms of percent inhibition was $67.63 \pm 3.18\%$ compared with pure FLF at $43.06 \pm 3.27\%$ 6 h after oral administration. There was a significant difference in the percent inhibition between FLF-TCMI and pure FLF ($P < 0.05$). The anti-inflammatory activity of FLF-TCMI was not significantly different than pure FLF (P 0.05). After 2, 4, and 6 h, this effect was found to be significant to pure FLF 1 h after oral administration ($P < 0.05$). The enhanced anti-inflammatory effects may be due to the fast absorption of FLF from TCMI. The presence of solubility enhancers (β-CD and Soluplus®) in the complex leads to higher solubility and biological activity. The anti-inflammatory activity of FLF-TCMI may be due to the inhibition of different mediators associated with inflammation, such as prostaglandins and pro-inflammatory cytokines (49).

CONCLUSION

The present research successfully demonstrated the formulation of FLF:β-CD and FLF:β-CD:Soluplus® inclusion complexes using SE and MI methods. Improved apparent stability constant (Kc) and complexation efficiency (CE) were observed for β-CD with the addition of Soluplus®, which indicates the formation of a stable complex. Soluplus® was positioned on the outer surface of the complex and showed improved solubility and release. The DSC and XRD techniques confirmed the transformation of the FLF state from crystalline to amorphous. The IR and NMR spectra revealed the formation of a stable complex *via* bridging between FLF and β-CD. The *in vivo* anti-inflammatory activity results revealed significantly enhanced biological activity in the animal model. Therefore, the results of our study support the use of Soluplus® as an auxiliary substance to improve drug solubility and dissolution.

FUNDING INFORMATION

COMPLIANCE WITH ETHICAL STANDARDS

The protocol for these studies was reviewed and approved by the "Animal Ethics Committee of King Saud University, Riyadh, Saudi Arabia (approval number KSU-SE-19-19)."

REFERENCES

1. Rubio L, Alonso C, Rodríguez G, Cocera M, López-Iglesias C, Coderch L, et al. Bicellar systems as new delivery strategy for topical application of flufenamic acid. Int J Pharm. 2013;444(1–2):60–9.

2. Alshehri S, Shakeel F, Ibrahim M, Elzayat E, Altamimi M, Shazly G. Influence of the microwave technology on solid dispersions of mefenamic acid and flufenamic acid. PLoS One. 2017;12(7):e0182011.

3. Baek JS, Yeo EW, Lee YH, Tan NS, Loo SCJ. Controlled-release nanoencapsulating microcapsules to combat inflammatory diseases. Drug Des Dev Ther. 2017;11:1707–17.

4. Mohamed AA, Matijevic E. Preparation and characterization of uniform particles of flufenamic acid and its calcium and barium salts. J Colloid Interface Sci. 2012;381(1):198–201.

5. Badran M. Formulation and in vitro evaluation of flufenamic acid loaded deformable liposomes for improved skin delivery. Digest J Nanomat Biostr. 2014;9(1):83–91.

6. Abignente E, DeCaprariis P. Flufenamic acid: analytical profiles of drug substances, New York: Academic Press, Inc., 313–346 (1982).

7. Alshehri S, Shakeel F. Solubility measurement, thermodynamics and molecular interactions of flufenamic acid in different neat solvents. J Mol Liq. 2017;240:447–53.

8. Abignente E, Caprariis P. Flufenamic Acid. Analytical Profiles of Drug Substances11, 1982, PP- 313-346.

9. Aronson JK. Meyler's side effects of analgesics and anti-inflammatory drugs. Elsevier, 2009 ISBN 9780080932941.

10. Ibolya F, Gyeresi A, Szabo-Revesz P, Aigner Z. Solid dispersion of flufenamic acid with PEG 4000 and PEG 6000. Farmacia. 2011;1(59):60–9.

11. Itai S, Nemoto M, Kouchiwa S, Murayama H, Nagai T. Influence of wetting factors on the dissolution behavior of flufenamic acid. Chem Pharm Bull. 1985;33:5464–73.

12. Nechipadappu SK, Tekuri V, Trivedi DR. Pharmaceutical co-crystal of flufenamic acid: synthesis and characterization of two novel drug-drug co-crystal. J Pharm Sci. 2017;106:1384–90.

13. Belhocine Y, Bouhadiba A, Rahim M, Nouar L, Djilani I, Khatmic DE. Inclusion complex formation of β-Cyclodextrin with the nonsteroidal anti-inflammatory drug flufenamic acid: computational study. Macroheterocycles. 2018;11(2):203–9.

14. Soares-Sobrinho JL. Soares MFdLR, Rolim-Neto PJ, Torres-Labandeira J. Physicochemical study of solid-state benznidazole–cyclodextrin complexes. J Thermal Anal Cal. 2011;106(2):319–25.

15. Brewster ME, Loftsson T. Cyclodextrins as pharmaceutical solubilizers. Adv Drug Deliv Rev. 2007;59(7):645–66.

16. Moura LCS, Batista DRMR, Honorato SB, Ayala AP, Morais WA, Barbosa EG, et al. Effect of hydroxypropyl methylcellulose on beta cyclodextrin complexation of praziquantel in solution and in solid state. J Incl Phenom Macrocycl Chem. 2016;85:151–60.

17. Mennini N, Maestrelli F, Cirri M, Mura P. Analysis of physicochemical properties of ternary systems of oxaprozin with randomly methylated-ß-cyclodextrin and L-arginine aimed to improve the drug solubility. J Pharm Biomed Anal. 2016;129:350–8.

18. Srivalli KMR, Mishra B. Improved aqueous solubility and antihypercholesterolemic activity of ezetimibe on formulating with Hydroxypropyl-β-cyclodextrin and hydrophilic auxiliary substances. AAPS Pharm Sci Tech. 2016;17(2):272–83.

19. Alvarez-Rivera F, Fernandez-Villanueva D, Concheiro A, &Alavez-Lorenzo, C. α-Lipoic acid in Soluplus® polymeric nanomicelles for ocular treatment of diabetes associated corneal diseases. J Pharm Sci. 2016;105:2855–63.

20. Taveira SF, Varela-Garcia A, Souza BS, Marreto RN, Pastor MM, Concheiro A, et al. Cyclodextrin-based poly(pseudo)rotaxanes for transdermal delivery of Carvedilol. Carbohyd Polymers. 2018;200:278–88.

21. Julia F. Alopaeus, Ellen Hagesaeher, IngunnTho. Micellisation mechanism and behaviour of Soluplus®–furosemide micelles: preformulation studies of an oral nanocarrier-based system. Pharmaceuticals. 2019;12(1):15.

22. Taupitz T, Dressman JB, Buchanan CM, Klein S. Cyclodextrin-water soluble polymer ternary complexes enhance the solubility and dissolution behaviour of poorly soluble drugs. Case example: itraconazole. Eur J Pharm Biopharm. 2013;83(3):378–87.

23. França MT, Pereira RN, Riekes MK, Pinto JMO, Stulzer HK. Investigation of novel supersaturating drug delivery systems of chlorthalidone: the use of polymer-surfactant complex as an effective carrier in solid dispersions. Eur J Pharm Sci. 2018;111:142–52.

24. Tao C, Huo T, Zhang Q, Song H. Effect of Soluplus® on the supersaturation and absorption of tacrolimus formulated as inclusion complex with dimethyl-β-cyclodextrin. Pharm Dev Technol. 2019;24(9):1076–82.

25. Thiry J, Krier F, Ratwatte S, Thomassin JM, Jerome C, Evrard B. Hot-melt extrusion as a continuous manufacturing process to form ternary cyclodextrin inclusion complexes. Eur J Pharm Sci. 2017;96:590–7.

26. Lorenzo-Veiga B, Sigurdsson HH, Loftsson T, Alvarez-Lorenzo C. Cyclodextrin–amphiphilic copolymer supramolecular assemblies for the ocular delivery of natamycin. Nanomaterials. 2019;9:745–63.

27. Marcos X, Perez-Casas S, Llovo J, Concheiro A, Alvarez-Lorenzo C. Poloxamer-hydroxyethyl cellulose-alpha-cyclodextrin supramolecular gels for sustained release of griseofulvin. Int J Pharm. 2016;500:11–9.

28. Medarević D, Kachrimanis K, Djuric Z, Ibric S. Influence of hydrophilic polymers on the complexation of carbamazepine

with hydroxypropyl-β-cyclodextrin. Eur J Pharm Sci. 2015;78:273–85.

29. Lim SM, Pang ZW, Tan HY, Shaikh M, Adinarayana G, Garg S. Enhancement of docetaxel solubility using binary and ternary solid dispersion systems. Drug Dev Ind Pharm. 2015;41(11):1847–55.

30. Higuchi T, Connors KA. Phase solubility techniques. Adv Anal Chem Instrum. 1965;4:117–212.

31. Patel M, Hirlekar R. Multicomponent cyclodextrin system for improvement of solubility and dissolution rate of poorly water soluble drug. Asian J Pharm Sci. 2019;14(1):104–15.

32. Wen X, Tan F, Jing Z, Iiu Z. Preparation and study of the 1:2 inclusion complex of carvedilol with β - cyclodextrin. J Pharm Biomed Anal. 2004;34:517–23.

33. Moneghini M, Zingone G, Zordi ND. Influence of microwave technology on the physical-chemical properties of solid dispersion with nimesulide. Powder Technol. 2009;195:259–63.

34. Suvarna V, Thorat S, Nayak U, Sherje A, Murahari M. Host-guest interaction study of Efavirenz with hydroxypropyl-β-cyclodextrin and L-arginine by computational simulation studies: preparation and characterization of supramolecular complexes. J Mol Liq. 2018;259:55–64.

35. Costa P, Sousa Lobo JM. Modeling and comparison of dissolution profiles. Eur J Pharm Sci. 2001;13(2):123–33.

36. Alshehri S, Imam SS, Altamimi MA, Jafar M, Hassan MZ, Hussain A, et al. Host-guest complex of β-cyclodextrin and pluronic F127 with Luteolin: physicochemical characterization, anti-oxidant activity and molecular modeling studies. J Drug Del Sci Tech. 2020;55:101356.

37. Thiry J, Kok MGM, Collard L, Frere A, Krier F, Fillet M, et al. Bioavailability enhancement of itraconazole-based solid dispersions produced by hot melt extrusion in the framework of the Three Rs rule. Eur J Pharm Sci. 2017;99:1–8.

38. Wada Y, Etoh Y, Ohira A, Kimata H, Koide T, Ishihama H, et al. Percutaneous absorbtion and anti-inflammatory activity of indomethacin in ointment. J Pharm Pharmcol. 1982;34:467–8.

39. Escribano E, Calpena AC, Queralt J, Obach R, Doménech J. Assessment of diclofenac permeation with different formulations: anti-inflammatory study of a selected formula. Eur J Pharm Sci. 2003;19:203–10.

40. Manca ML, Zaru M, Ennas G, Valenti D, Sinico C, Loy G, et al. Diclofenac-β-cyclodextrin binary systems: physicochemical characterization and in vitro dissolution and diffusion studies. AAPS Pharm Sci Tech. 2005;6(3):E464–72.

41. Bera H, Chekuri S, Sarkar S, Kumar S, Muvva NB, Mothe S, et al. Novel pimozide-β-cyclodextrin-polyvinyl pyrrolidone inclusion complexes for Tourette syndrome treatment. J Mol Liq. 2016;215:135–43.

42. Flufenamic acid. Drugbank. Available at: http://www.drugbank.ca/drugs/ DB02266. Accessed January 1, 2020.

43. Sherje AP, Kulkarni V, Murahari M, Nayak UY, Bhat P, Suvarna V, et al. Inclusion complexation of etodolac with hydroxypropyl-beta-cyclodextrin and auxiliary agents: formulation characterization and molecular modeling studies. Mol Pharm. 2017;14(4):1231–42.

44. Bajerski L, Rossi RC, Dias CL, Bergold AM, Froehlich PE. Development and validation of a discriminating in vitrodissolutionmethod for a poorly soluble drug, Olmesartanmedoxomil: comparison between commercial tablets. AAPS Pharm Sci Tech. 2010;11(2):637–44.

45. Ma B, Shen Y, Fan Z, Zheng Y, Sun H, Luo J, et al. Characterization of the inclusion complex of 16, 17α-epoxy progesterone with randomly methylated β-cyclodextrin in aqueous solution and in the solid state. J Incl Phenom Macrocycl Chem. 2011;69:273–80.

46. Zawar LR, Bari SB. Preparation, characterization and in vivo evaluation of antihyperglycemic activity of microwave generated repaglinide solid dispersion. Chem Pharm Bull. 2012;60(4):482–7.

47. Jansook P, Kulsirachote P, Loftsson T. Cyclodextrin solubilization of celecoxib: solid and solution state characterization. J Inclusion Phenom Mac Chem. 2018;90:75–88.

48. Ganza-González A, Vila-Jato JL, Anguiano-Igea S, Otero-Espinar FJ, Blanco-Méndez J. A proton nuclear magnetic resonance study of the inclusion complex of naproxen with β-cyclodextrin. Int J Pharm. 1994;106(3):179–85.

49. Alshehri S, Shakeel F, Elzayat E, Almeanazel O, Altamimi M, Shazly G, et al. Rat palatability, pharmacodynamics effect and bioavailability mefenamic acid formulations utilizing hot-melt extrusion technology. Drug Dev Ind Pharm. 2019;45:1610–6.